SUPPLEMENTARY INFORMATION

Decoding the Substrate Specificity Landscape of a Promiscuous Enzyme through Multi-Substrate Mutational Scanning.

Rosario Vanella[1, 2, *], Sean Boult [1,2,3], Christoph Küng[1, 2], Michael A. Nash[1, 2, 4, 5 *]

[1] Department of Chemistry, University of Basel, 4058 Basel, Switzerland
[2] Department of Biosystems Science and Engineering, ETH Zurich, 4058 Basel, Switzerland
[3] Department of Health Sciences and Technology, ETH Zürich; Zürich 8092, Switzerland
[4] National Center for Competence in Research (NCCR), Molecular Systems Engineering, 4058 Basel, Switzerland
[5] Swiss Nanoscience Institute, 4056 Basel, Switzerland

* Correspondence to: rosario.vanella@unibas.ch; michael.nash@unibas.ch

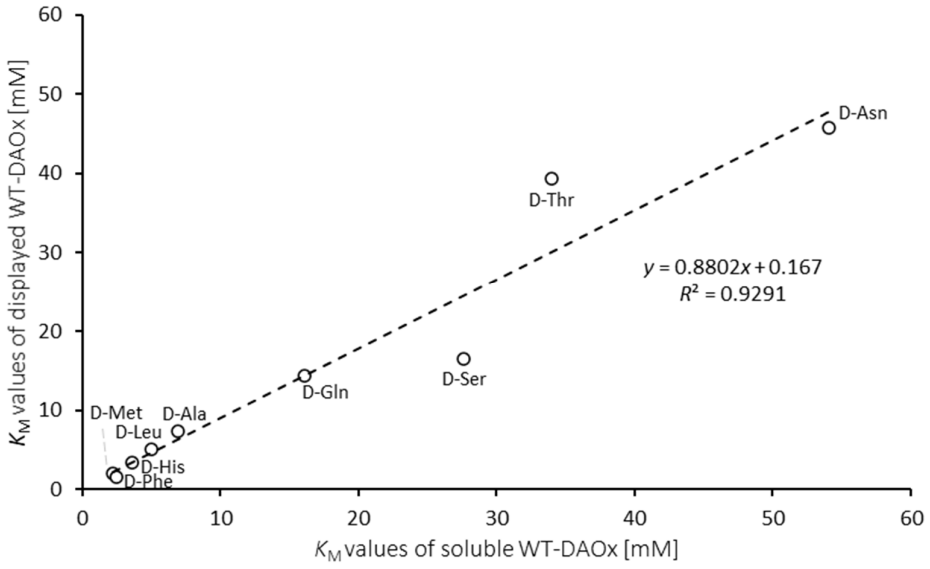

Supplementary Figure 1. Comparison of catalytic properties of soluble and yeast-displayed WT-DAOx.

Linear correlation between the K_M values towards nine different substrates of soluble and yeast displayed wild type DAOx. K_M values for each substrate tested both with displayed and soluble DAOx are reported in Supplementary table 1. Dashed line: linear regression; R^2: coefficient of determination. Data points represent mean values obtained from n = 3 independently measured samples from the same soluble and yeast-displayed enzyme preparation. Source data are provided as a Source Data file.

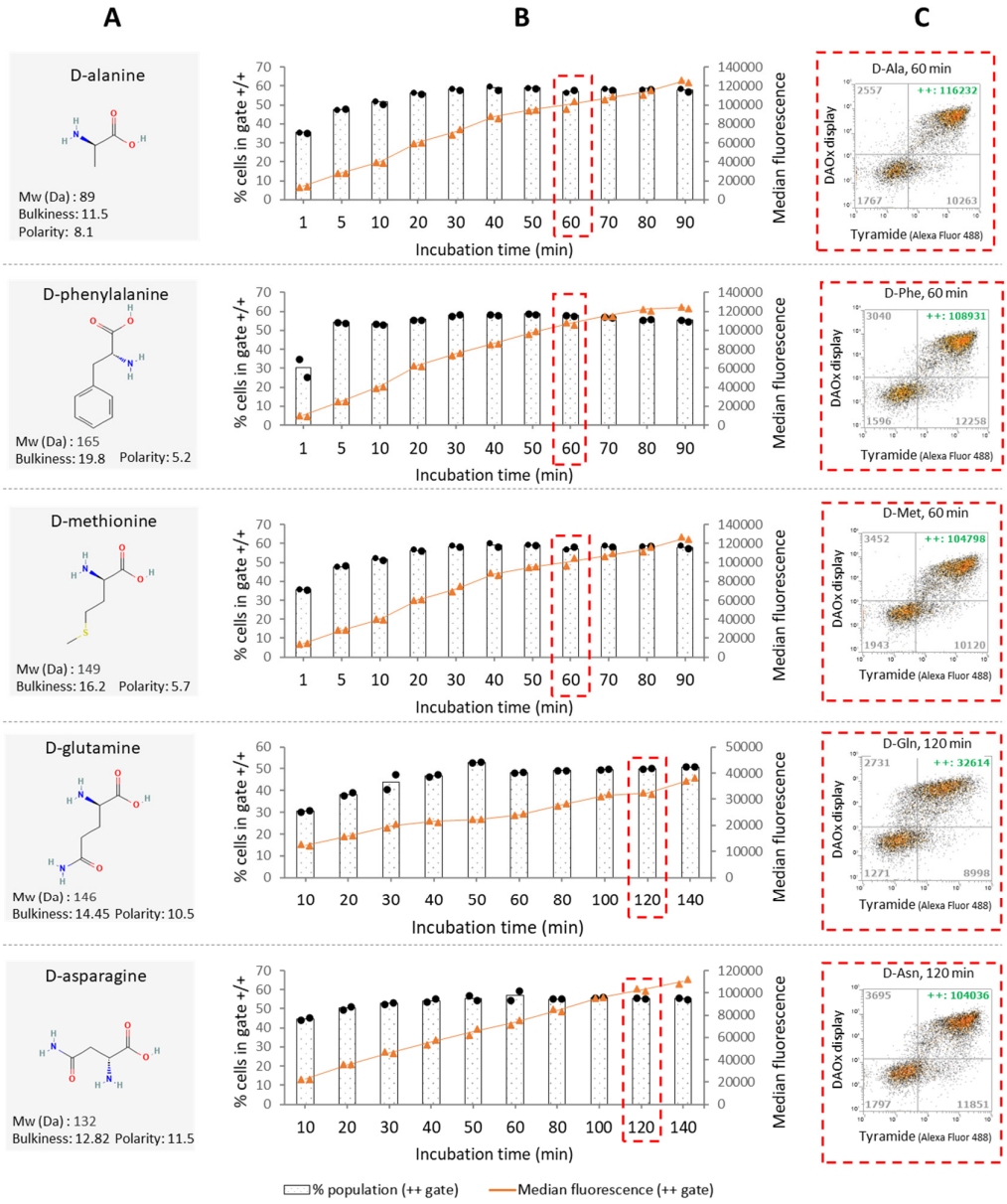

Supplementary Figure 2. Time-course tyramide assay of yeast displayed WT-DAOx

(**A**) Name, chemical structure and information about each of the five DAOx substrates used in the EP-Seq workflow. (**B**) Time course tyramide assay with yeast cells displaying wild type DAOx and five different D-amino acid substrates at an initial concentration equal to K_M. For each substrate, a different range of incubation time intervals was chosen based on the calculated k_{cat}. D-alanine, D-phenylalanine, and D-methionine (with k_{cat} between 59 and 74 s^{-1}) were incubated from 1 to 90 minutes for a total of 9 or 10 time points. D-glutamine and D-asparagine (with k_{cat} of 11 and 18 s^{-1}) were incubated for 10 to 140 minutes for a total of 10 time points. Per substrate, the final selected incubation time point used in the deep mutational scanning tyramide screening of the DAOx mutant library is highlighted by the dashed red. The selected time points ensure tyramide signal acquisition close to saturation levels for each amino acid, maximizing the sensitivity of the assay. Each datapoint of the assay was measured from two independent reactions from the same cell preparation. Source data are provided as a Source Data file. (**C**) A raw flow cytometry plot illustrating the population shift along the DAOx display and tyramide signal axis per each substrate and each selected condition is shown.

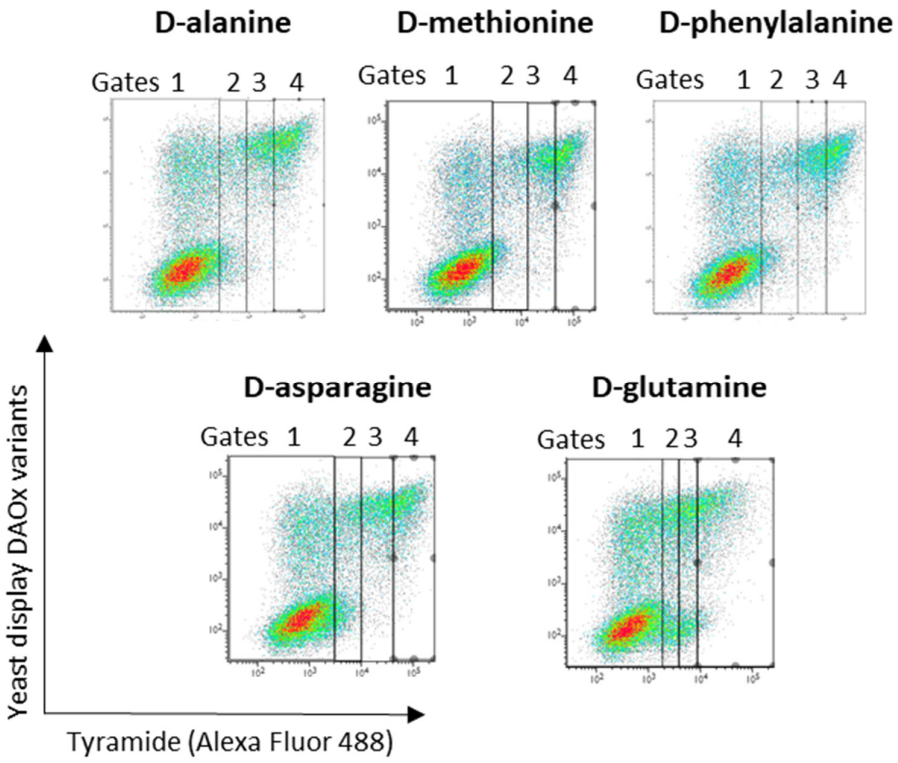

Supplementary Figure 3. FACS gating strategy for each of the five EP-Seq tyramide assays performed in the study.

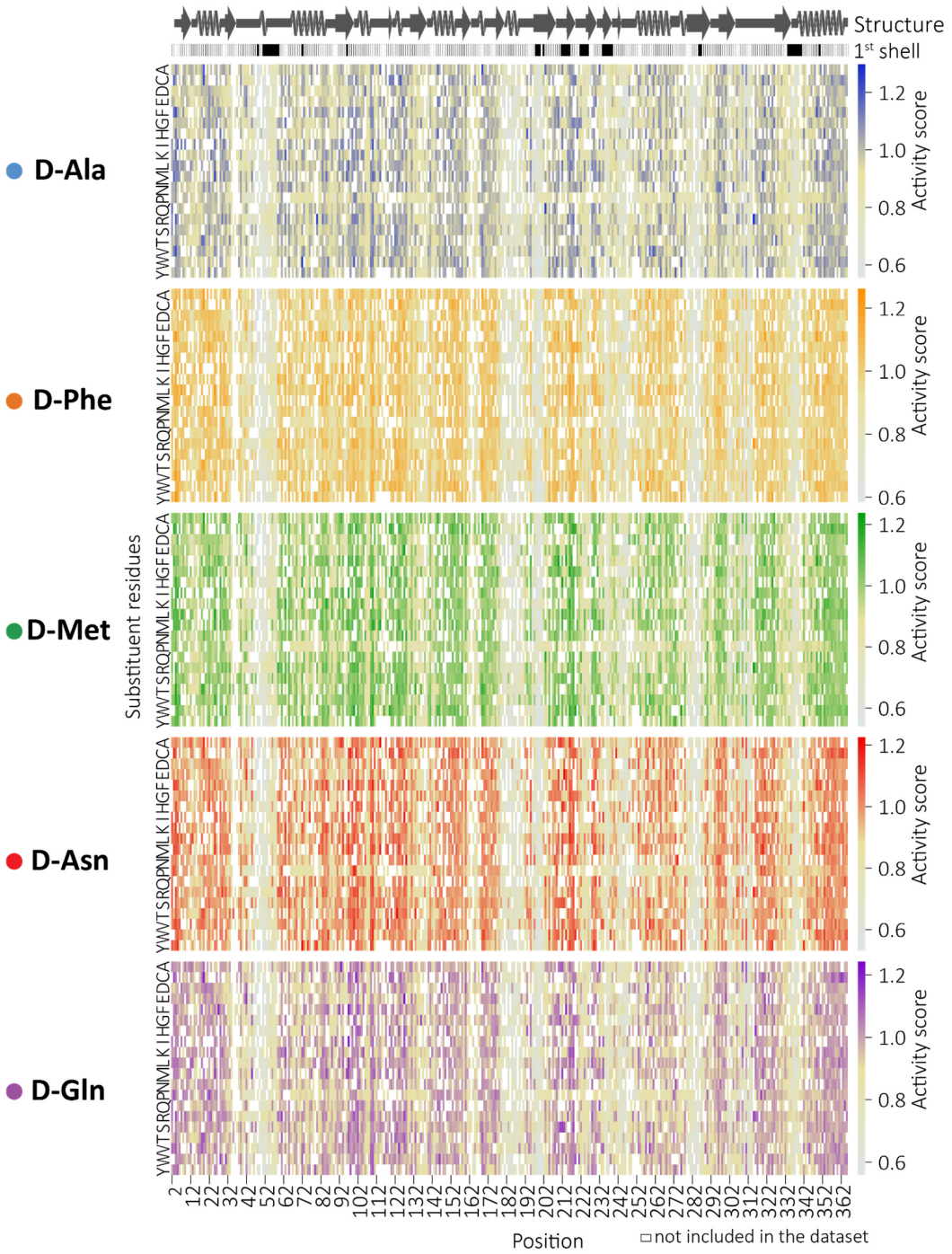

Supplementary Figure 4. DAOx single mutant activity scores across five substrates.

Heatmaps displaying EP-Seq activity fitness scores for all single missense mutations screened with each of the five substrates. The intensity of the color on the heatmap reflects the relative impact of each mutation on enzymatic activity for the respective substrate. Source data are provided as a Source Data file.

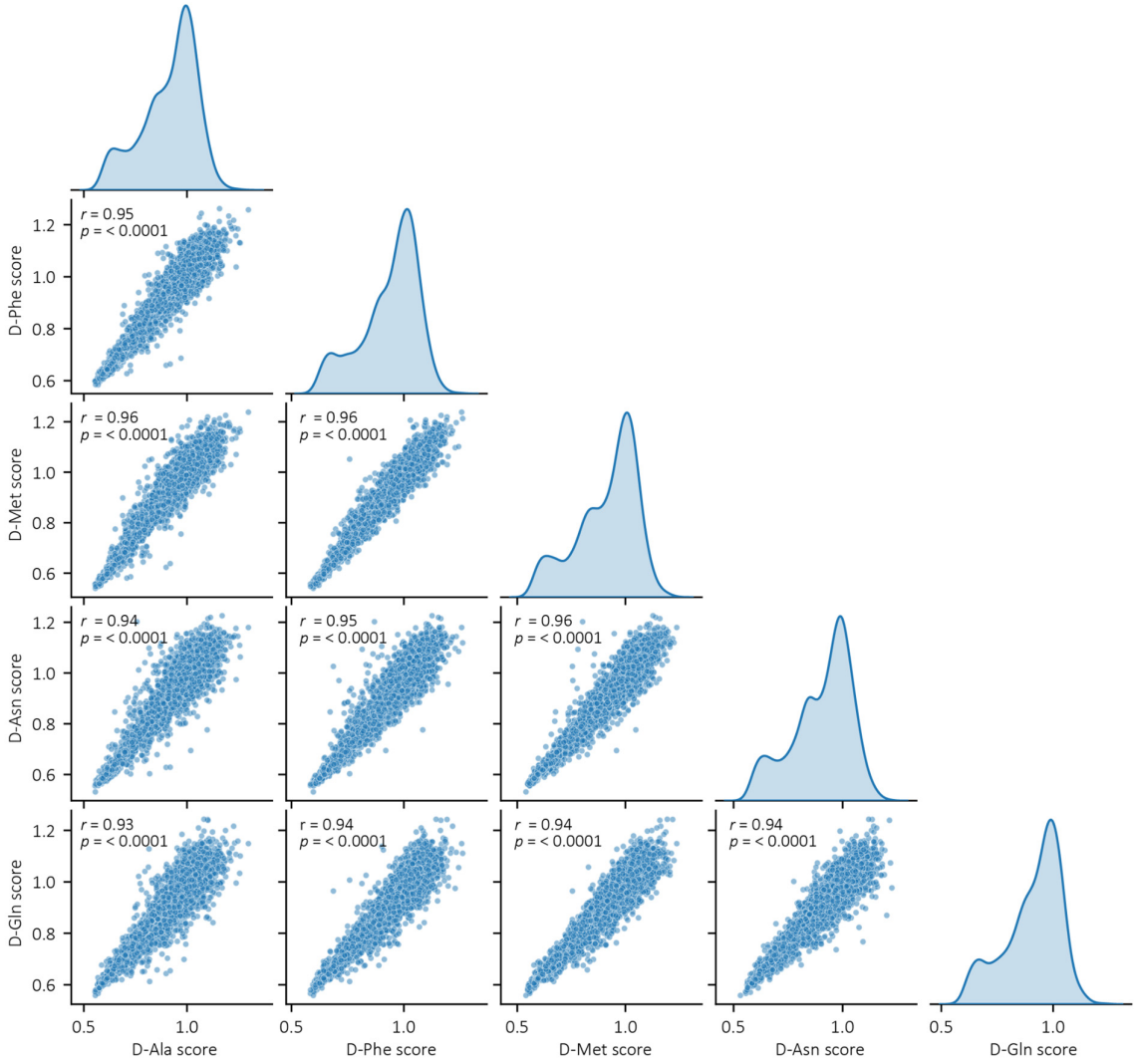

Supplementary Figure 5. Comparison of consensus DAOx activity fitness scores across five substrate screenings.

Linear regression analyses (Pearson's *r*, two-tailed) were performed to compare the activity fitness scores from EP-Seq screenings using different DAOx substrates. Each plot represents the relationship between two distinct screening datasets. Pearson's r values indicate the degree of concordance between the datasets. Source data are provided as a Source Data file.

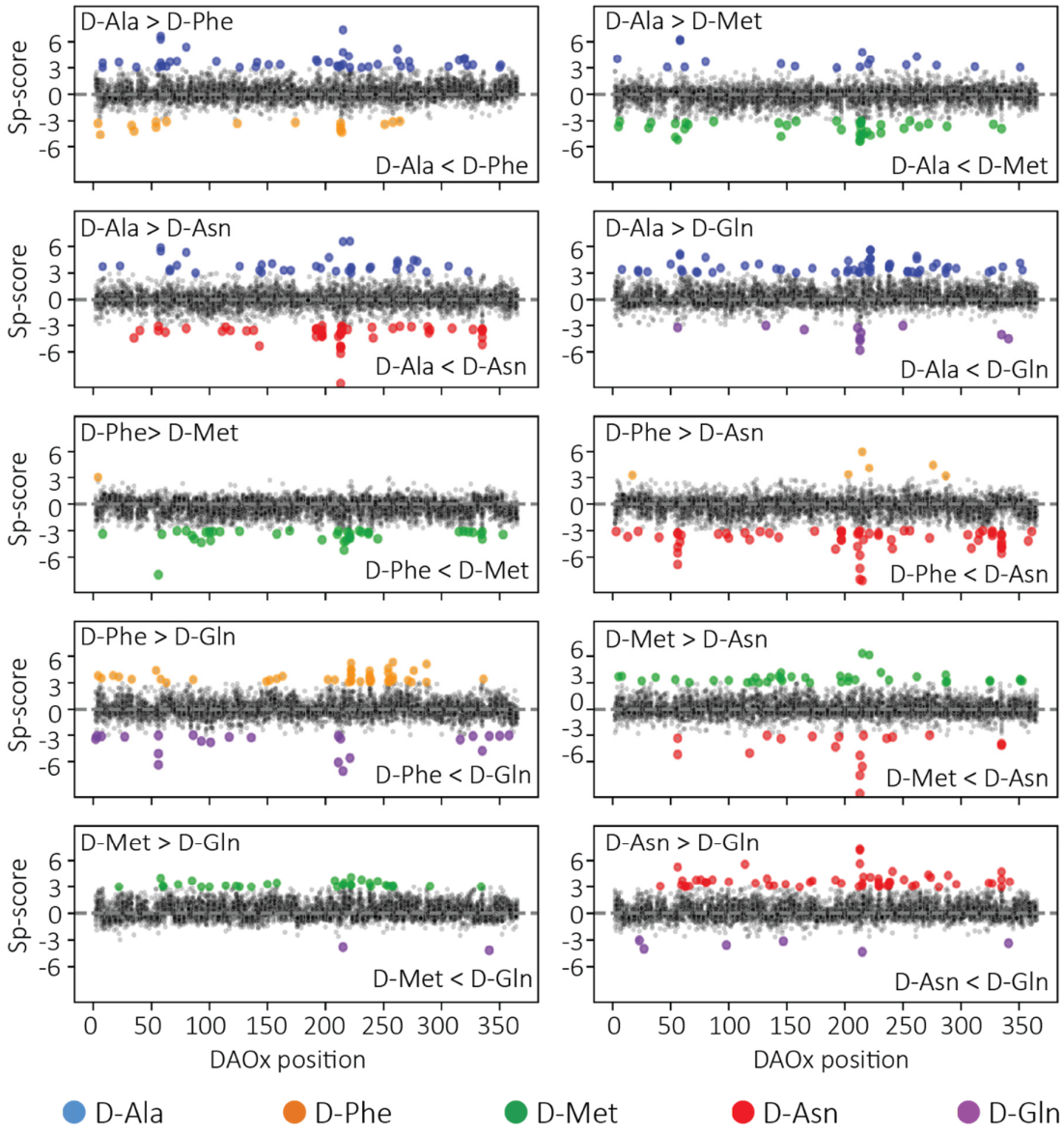

Supplementary Figure 6. Identification and localization of substrate-specific mutations in DAOx.

Scatter plots of Sp-scores per position of DAOx for each variant enzyme and across all possible pairwise comparisons of EP-Seq screenings results performed with different substrates. Colored dots indicate variants with Sp-scores above 3 or below -3, representing substrate-specific mutations. Substrate-specific mutations are color-coded as follows: D-Ala-specific variants in blue, D-Phe-specific in orange, D-Met-specific in green, D-Asn-specific in red, and D-Gln-specific in violet. This color scheme is consistently used throughout the manuscript to denote substrate-specific mutations. Source data are provided as a Source Data file.

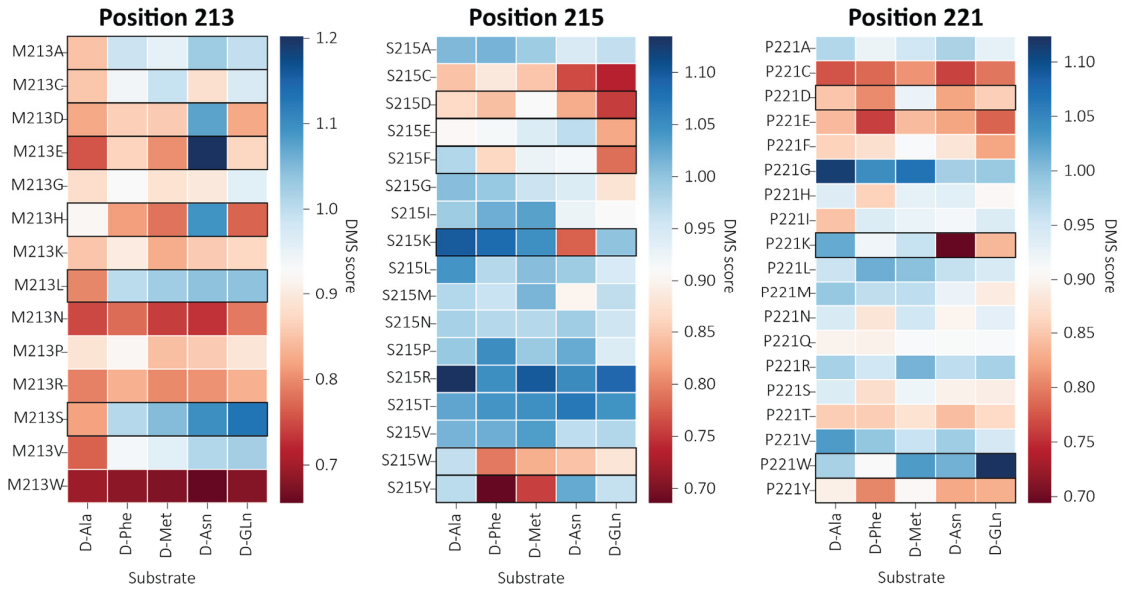

Supplementary Figure 7. DAOx positions 213, 215 and 221 play a general role in substrate specificity.

Heatmap overview of EP-Seq scores for single-point mutants at positions 213, 215 and 221 tested across all five substrates (D-Ala, D-Phe, D-Met, D-Asn, and D-Gln), highlighting position-specific effects on substrate preference. Source data are provided as a Source Data file.

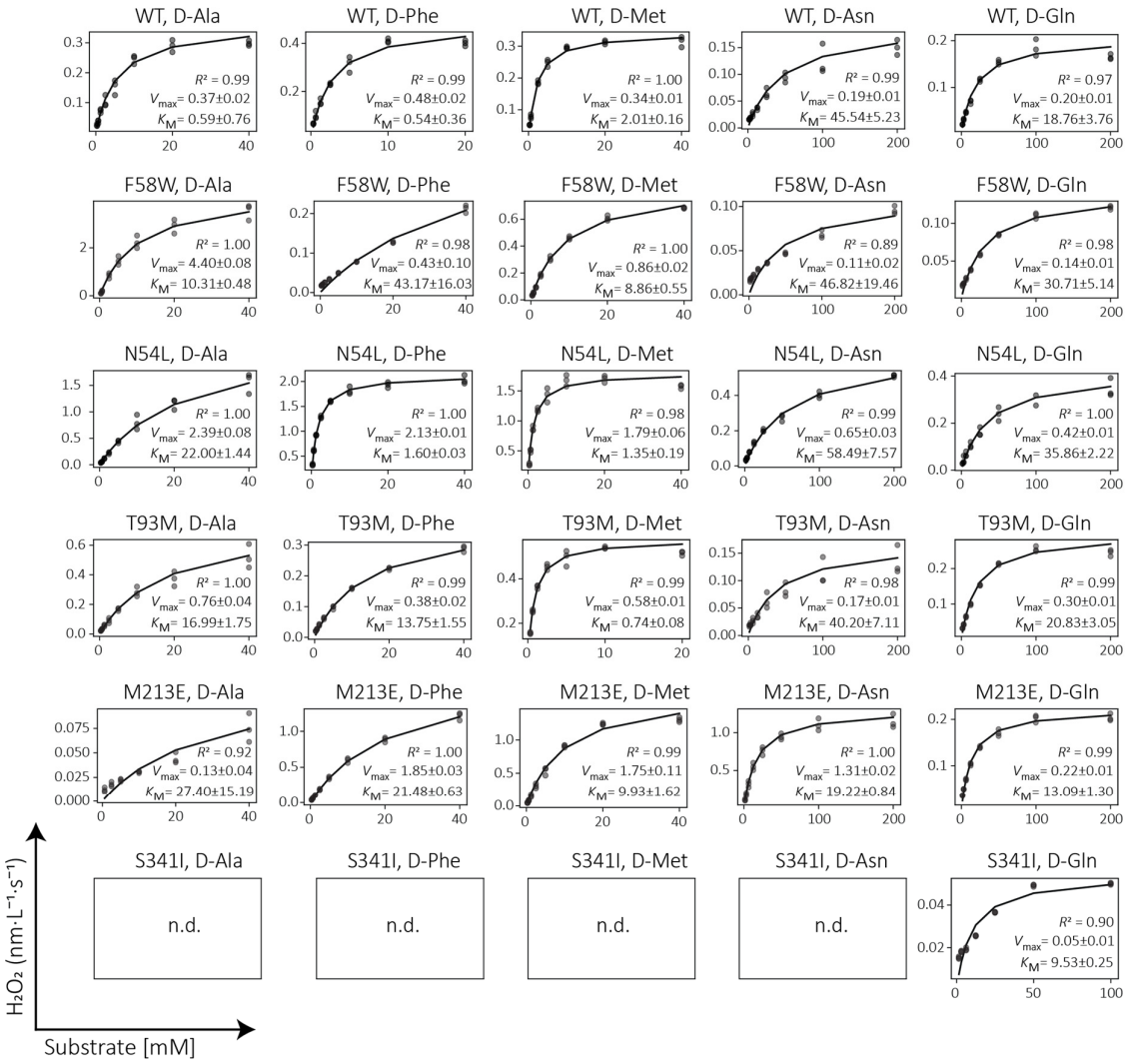

Supplementary Figure 8. Kinetic profiles of soluble WT and DAOx variants.

Michaelis–Menten plots showing initial rates of H_2O_2 formation as a function of substrate concentration for wild-type (WT) and five DAOx variants. Soluble proteins were expressed in *E. coli* NiCo21(DE3) and purified using affinity and size exclusion chromatography to ensure high and comparable purity across all enzymes. Enzyme concentrations used for kinetic measurements were: 0.25 nM WT, 2 nM N54L, 2 nM F58W, 5 nM T93M, 5 nM S341I, and 1 nM M213E. n.d. (not detected) indicates no measurable activity, with signal below the detection limit of the assay. Points represent independent measurements from the same enzyme preparation (n = 3 per substrate concentration). The curve shows the nonlinear regression fit to the Michaelis–Menten equation performed on the mean values. Source data are provided as a Source Data file.

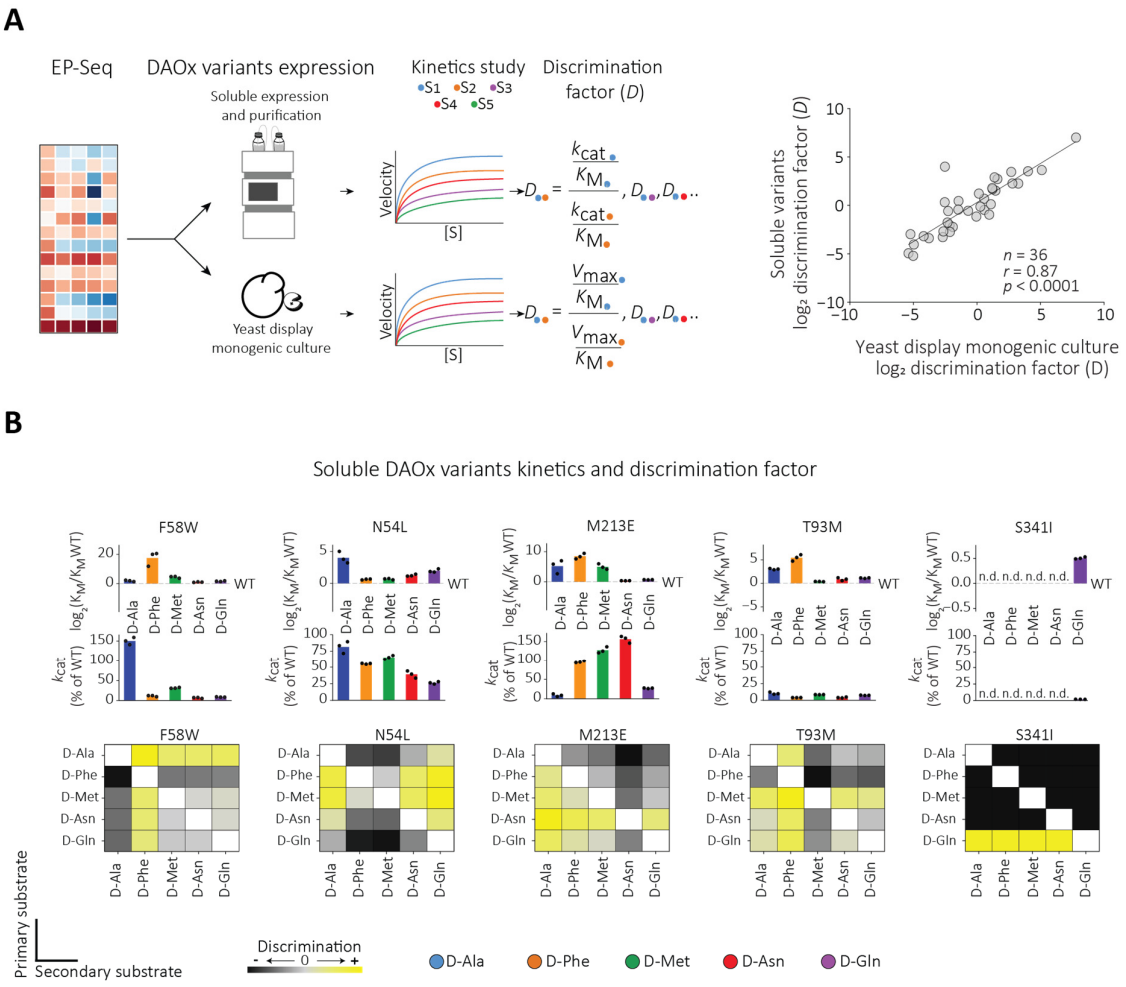

Supplementary Figure 9. Validation and Analysis of Soluble Variants' D-Factors.

(**A**) Workflow illustrating the D-factor validation process: substrate-specific single mutants identified through EP-Seq were expressed both as monoclonal yeast display variants and as soluble proteins in *E. coli* (left). Catalytic efficiencies (k_{cat}/K_M) were determined for the soluble forms across all five substrates and compared with their yeast-displayed counterparts to assess consistency between formats (right). Dashed line: linear regression; *r*: Pearson correlation coefficients, n: number of datapoints, *p*: p-values two-tailed. (**B**)(Top) Catalytic profiles of selected variants expressed as soluble enzymes. Relative changes in k_{cat} and V_{max} values compared to the wild-type enzyme for each of the five substrates, illustrating how specificity is tuned through alterations in substrate affinity and catalytic turnover. Values from $n = 3$ independently measured samples from the same enzyme preparation. (Bottom) Heatmaps of substrate discrimination factor for all pairwise combinations of primary (y-axis) and secondary (x-axis) substrates, calculated as the catalytic efficiency (k_{cat} / K_M) for the primary substrate divided by that for the secondary substrate. n.d. (not detected) indicates no measurable activity, with signal below the detection limit of the assay. Values from $n = 3$ independently measured samples from the same enzyme preparation. Source data are provided as a Source Data file.

Supplementary Table 1. Comparison of kinetic features between yeast-displayed and soluble WT-DAOx.

Michaelis-Menten constant K_M (mean ± standard deviation) experimentally assayed for the yeast displayed and soluble form of the WT-DAOx. Coefficients of determination (R^2) for each of the fitted datasets are reported.

Substrate	Soluble DAOx K_M [mM]	R^2	Surface displayed DAOx K_M [mM]	R^2
D-Ala	6.965 ± 0.4003	0.9937	7.316 ± 0.2816	0.9973
D-Met	2.214 ± 0.1608	0.9850	2.039 ± 0.1455	0.9851
D-Phe	2.497 ± 0.1033	0.9950	1.507 ± 0.05914	0.9947
D-Gln	16.12 ± 0.8415	0.9961	14.42 ± 0.8434	0.9950
D-His	3.612 ± 0.1662	0.9942	3.406 ± 0.2003	0.9923
D-Thr	34.01 ± 2.745	0.9883	39.38 ± 1.548	0.9975
D-Asn	54.05 ± 4.683	0.9958	45.82 ± 1.488	0.9990
D-Ser	27.58 ± 2.755	0.9813	16.47 ± 0.6280	0.9967
D-Leu	5.021 ± 0.2623	0.9940	4.991 ± 0.1093	0.9990

Supplementary Table 2. Sorted cells, Illumina reads, and median fluorescence values per sorting gate.

Experiment	Bin	# Illumina reads	# Sorted cells	Median fluorescence
D-alanine screening Replicate 1	1	44100714	3951383	672.5
	2	37370660	425024	4580
	3	42886950	407658	17367
	4	41175573	485113	54275.125
D-alanine screening Replicate 2	1	49230428	7020636	504.5
	2	38379877	468261	4764.125
	3	37319082	625693	17491.625
	4	40512560	641907	52822.75
D-methionine screening Replicate 1	1	47604620	8290439	741
	2	36257935	1078896	5076
	3	33684162	1190286	26548
	4	34336748	1125873	71588
D-methionine screening Replicate 2	1	42408681	7565518	735
	2	35254873	971169	4986
	3	34252436	1032611	26473
	4	35238485	923507	71469
	1	46910569	8343237	714

D-phenylalanine screening Replicate 1	2	28055538	1117236	5198
	3	27966355	1276152	28036
	4	25871098	1152820	75211
D-phenylalanine screening Replicate 2	1	37163633	6448964	690
	2	38860381	867477	5105
	3	32718506	870761	26350
	4	32567797	724807	70094
D-asparagine screening Replicate 1	1	42675792	6194903	744
	2	42086369	887066	4940
	3	31855534	920042	21483
	4	43640442	778517	70691
D-asparagine screening Replicate 2	1	35894362	6479013	773
	2	33143311	835295	4836
	3	27876393	939669	22120
	4	30558626	840663	71013
D-glutamine screening Replicate 1	1	41006142	6663201	484
	2	38484786	912438	2650
	3	43725266	925690	5522
	4	43218258	950405	17090
	1	28002452	5918410	485

D-glutamine screening Replicate 2	2	40842045	872992	2664
	3	30320723	897982	5534
	4	32201970	947327	17639

Supplementary Table 3. Linear regression correlation and fitness metrics per subpopulation in EP-Seq screening.

Pearson correlation coefficient (PCCR) *r* of the linear regression between experimental replicates in **Fig. 2**. Details on the composition of the single mutant variants per each EP-Seq screen and substrate. Specifically, number of missense variants, percentage of total, median score; number of nonsense variants and average activity score with standard deviation; number of synonymous variants and average activity score with standard deviation.

D-alanine	
PCC (*r*)	0.93
# missense variants # (% tot, median score)	6377 (92.2%, -0.33)
# nonsense variants (mean score ± SD)	332 (-0.60±0.11)
# synonymous variants (mean score ± SD)	298 (-0.000565±0.064)
D-phenylalanine	
PCC (*r*)	0.96
# missense variants # (% tot, median score)	6400 (92.5%, -0.28)
# nonsense variants (mean score ± SD)	333 (-0.53±0.09)
# synonymous variants (mean score ± SD)	300 (-0.000546±0.054)
D-methionine	
PCC (*r*)	0.96
# missense variants # (% tot, median score)	6414 (92.7%, -0.28)
# nonsense variants (mean score ± SD)	333 (-0.63±0.11)
# synonymous variants (mean score ± SD)	301 (-0.00368±0.052)
D-glutamine	
PCC (r)	0.94
# missense variants # (% tot, median score)	6426 (92.9%, -0.35)
# nonsense variants (mean score ± SD)	332 (-0.55±0.10)
# synonymous variants (mean score ± SD)	301 (-0.00232±0.051)
D-asparagine	
PCC (*r*)	0.93
# missense variants # (% tot, median score)	6379 (92.2%, -0.34)
# nonsense variants (mean score ± SD)	332 (-0.61±0.11)
# synonymous variants (mean score ± SD)	302 (-0.0007±0.061)
All datasets (variants shared by all datasets)	
# missense variants # (% tot, mean score)	5821 (84.2%, -0.31±0.05)
# nonsense variants (mean score ± SD)	316 (-0.58±0.05)
# synonymous variants (mean score ± SD)	281 (-0.0026±0.0350)

Supplementary Table 4. Most selective DAOx variants per substrate identified by EP-Seq.

For each variant, the table reports the distance of the mutation from the catalytic site, the identities of the primary and secondary substrates, the measured activity scores on each substrate, and the Sp-score between the primary and secondary substrates.

		Substrate		Activity score					
DAOx variant	**Distance to catalytic site (Å)**	**Primary**	**Secondary**	**D-Ala**	**D-Phe**	**D-Met**	**D-Asn**	**D-Gln**	**Sp-score**
S215Y	7.28	**D-Ala**	D-Phe	0.97	0.69	0.76	1.03	0.96	7.33
F58Y	2.21	**D-Ala**	D-Phe	0.92	0.66	0.64	0.63	0.65	6.65
P221K	7.10	**D-Ala**	D-Asn	1.02	0.92	0.96	0.69	0.84	6.57
S215K	7.28	**D-Ala**	D-Asn	1.10	1.08	1.05	0.78	1.00	6.54
F58W	2.21	**D-Ala**	D-Phe	0.90	0.66	0.62	0.63	0.64	6.30
F58Y	2.21	**D-Ala**	D-Met	0.92	0.66	0.64	0.63	0.65	6.25
F58W	2.21	**D-Ala**	D-Met	0.90	0.66	0.62	0.63	0.64	6.13
F58Y	2.21	**D-Ala**	D-Asn	0.92	0.66	0.64	0.63	0.65	5.86
A222M	6.74	**D-Ala**	D-Gln	0.99	0.91	0.85	0.80	0.70	5.60
A222N	6.74	**D-Ala**	D-Gln	1.13	1.09	0.95	0.95	0.84	5.56
M213E	2.51	**D-Asn**	D-Met	0.76	0.87	0.80	1.20	0.87	9.61
M213E	2.51	**D-Asn**	D-Ala	0.76	0.87	0.80	1.20	0.87	9.57
S215Y	7.28	**D-Asn**	D-Phe	0.97	0.69	0.76	1.03	0.96	8.66
M213E	2.51	**D-Asn**	D-Phe	0.76	0.87	0.80	1.20	0.87	8.51
M213H	2.51	**D-Asn**	D-Met	0.92	0.81	0.78	1.09	0.77	7.54
M213E	2.51	**D-Asn**	D-Gln	0.76	0.87	0.80	1.20	0.87	7.32
M213H	2.51	**D-Asn**	D-Phe	0.92	0.81	0.78	1.09	0.77	7.28
M213H	2.51	**D-Asn**	D-Gln	0.92	0.81	0.78	1.09	0.77	7.18
T56H	3.47	**D-Asn**	D-Phe	0.81	0.71	0.76	0.97	0.74	6.84
S215Y	7.28	**D-Asn**	D-Met	0.97	0.69	0.76	1.03	0.96	6.55
T56M	3.47	**D-Met**	D-Phe	0.83	0.76	1.05	0.93	1.01	7.99
S215K	7.28	**D-Met**	D-Asn	1.10	1.08	1.05	0.78	1.00	6.32
P221K	7.10	**D-Met**	D-Asn	1.02	0.92	0.96	0.69	0.84	6.13
M213S	2.51	**D-Met**	D-Ala	0.82	1.01	1.05	1.10	1.13	5.39
M213L	2.51	**D-Met**	D-Ala	0.80	1.00	1.02	1.04	1.04	5.28
S216G	10.84	**D-Met**	D-Phe	1.01	1.03	1.21	1.11	1.04	5.20

T56M	3.47	**D-Met**	D-Ala	0.83	0.76	1.05	0.93	1.01	5.18
N54I	2.58	**D-Met**	D-Ala	0.69	0.86	0.90	0.75	0.77	4.89
Y145W	17.59	**D-Met**	D-Ala	0.92	1.06	1.13	0.98	1.04	4.79
D214F	6.73	**D-Met**	D-Ala	0.98	1.09	1.18	1.11	1.18	4.72
S215K	7.28	**D-Phe**	D-Asn	1.10	1.08	1.05	0.78	1.00	5.99
H258W	11.57	**D-Phe**	D-Gln	1.06	1.23	1.10	1.10	0.97	5.32
A222N	6.74	**D-Phe**	D-Gln	1.13	1.09	0.95	0.95	0.84	5.22
A287H	8.78	**D-Phe**	D-Gln	1.00	1.07	0.95	0.88	0.82	5.10
R254W	10.28	**D-Phe**	D-Gln	1.03	1.15	1.07	1.02	0.93	4.63
R6A	32.00	**D-Phe**	D-Ala	0.86	1.09	0.99	0.95	1.02	4.59
A222H	6.74	**D-Phe**	D-Gln	0.91	0.98	0.91	0.81	0.76	4.52
E276F	17.89	**D-Phe**	D-Asn	1.10	1.20	1.06	0.96	0.98	4.47
A222M	6.74	**D-Phe**	D-Gln	0.99	0.91	0.85	0.80	0.70	4.41
N54L	2.58	**D-Phe**	D-Gln	0.70	0.89	0.81	0.74	0.67	4.39
S215Y	7.28	**D-Gln**	D-Phe	0.97	0.69	0.76	1.03	0.96	7.06
T56M	3.47	**D-Gln**	D-Phe	0.83	0.76	1.05	0.93	1.01	6.36
C211S	5.99	**D-Gln**	D-Phe	1.00	0.90	0.99	1.07	1.14	6.08
M213S	2.51	**D-Gln**	D-Ala	0.82	1.01	1.05	1.10	1.13	5.81
P221W	7.10	**D-Gln**	D-Phe	0.98	0.91	1.03	1.01	1.12	5.60
T56Q	3.47	**D-Gln**	D-Phe	0.90	0.83	0.90	1.03	1.03	5.09
S335K	2.07	**D-Gln**	D-Phe	0.77	0.81	0.94	0.93	0.99	4.78
M213V	2.51	**D-Gln**	D-Ala	0.77	0.94	0.96	1.01	1.02	4.73
M213L	2.51	**D-Gln**	D-Ala	0.80	1.00	1.02	1.04	1.04	4.51
S341I	10.55	**D-Gln**	D-Ala	0.81	0.95	0.83	0.88	1.06	4.51

Supplementary Table 5. Kinetic profiles of yeast-displayed WT and DAOx variants.

Kinetic parameters (K_M and V_{max}) provided as mean value ± standard deviation for each yeast-displayed DAOx variant tested individually against the five substrates used in this study. n.d. (not detected) indicates values that were not measurable due to either the absence of detectable activity or unreliable fitting of the kinetic data. WT-DAOx was measured in parallel with each variant. V_{max} values for each variant were normalized to their respective expression levels, as determined by immunostaining, prior to being reported in the table for comparison. The WT reference is shown at the top of each group of variants that use it as a reference.

DAOx variants (yeast display)	Substrate									
	D-alanine		D-phenylalanine		D-methionine		D-asparagine		D-glutamine	
	K_M [mM]	V_{max} (nM/sec)	K_M [mM]	V_{max} (nM/sec)	K_M [mM]	V_{max} (nM/sec)	K_M [mM]	V_{max} (nM/sec)	K_M [mM]	V_{max} (nM/sec)
WT_1	2.31±0.72	1.94±0.23	0.45±0.07	1.99±0.14	0.49±0.01	2.04±0.03	9.66±0.35	0.93±0.03	7.94±0.32	0.75±0.01
N54I	16.05±1.43	0.54±0.03	0.85±0.04	0.67±0.0	0.49±0.02	0.75±0.01	21.05±2.62	0.21±0.0	10.6±0.21	0.23±0.0
N54L	22.24±0.91	0.76±0.0	0.83±0.02	0.65±0.01	0.91±0.25	0.56±0.0	26.04±0.58	0.16±0.01	25.11±0.86	0.14±0.0
T56H	7.15±0.25	0.7±0.0	16.03±0.22	1.34±0.01	3.59±0.16	0.95±0.02	22.77±0.68	0.76±0.02	23.93±1.37	0.24±0.01
T56M	12.68±0.68	1.1±0.02	15.18±0.34	1.2±0.04	0.53±0.01	1.09±0.01	31.44±8.38	0.64±0.0	7.81±0.8	0.51±0.02
T56Q	11.83±2.53	1.22±0.04	7.1±0.57	1.37±0.03	1.83±0.12	1.22±0.04	10.27±1.97	0.61±0.05	8.29±0.63	0.55±0.01
F58W	7.26±0.05	1.44±0.01	65.79±27.12	0.3±0.12	5.5±0.13	0.33±0.0	47.88±0.57	0.03±0.0	20.56±1.07	0.08±0.0
T93M	10.8±0.26	0.97±0.01	17.01±1.03	0.83±0.03	0.37±0.02	0.71±0.0	32.21±10.35	0.22±0.01	19.62±0.95	0.38±0.01
I197S	1.96±0.09	0.52±0.02	2.16±0.12	1.23±0.06	0.69±0.05	0.89±0.03	14.71±0.1	0.74±0.01	10.97±0.9	0.45±0.02
M213D	55.9±4.75	0.35±0.02	28.24±0.6	1.09±0.03	4.37±0.03	0.61±0.0	8.36±1.69	0.53±0.01	5.02±0.55	0.07±0.0
M213E	n.d.	n.d.	10.34±3.64	1.07±0.2	9.72±2.84	0.99±0.18	8.1±1.88	0.61±0.12	12.37±0.59	0.14±0.0
M213H	10.89±2.38	1.57±0.08	5.78±0.11	1.29±0.01	4.93±0.22	1.05±0.0	11.38±0.38	1.0±0.01	11.69±0.64	0.22±0.01
S215Y	2.08±0.12	0.89±0.0	14.84±0.05	0.71±0.0	2.07±0.11	0.59±0.0	6.39±0.32	0.58±0.01	8.53±0.24	0.34±0.0
A222M	4.44±0.26	1.05±0.08	1.5±0.21	1.02±0.1	2.43±0.04	0.86±0.03	21.11±0.54	0.27±0.01	26.91±0.41	0.17±0.0
H258W	6.51±0.5	1.72±0.07	0.55±0.01	1.42±0.02	1.34±0.05	1.59±0.01	11.15±0.32	0.46±0.01	18.08±0.07	0.45±0.0
E276F	4.48±0.81	2.47±0.16	0.77±0.1	2.36±0.1	0.91±0.1	2.43±0.06	18.14±1.65	1.0±0.0	13.9±1.33	0.81±0.02
S335K	n.d.	n.d.	6.93±0.03	0.39±0.0	1.47±0.0	0.71±0.0	37.57±0.65	0.57±0.0	10.41±0.27	0.43±0.0
S341I	n.d.	n.d.	n.d.	n.d.	n.d.	n.d.	n.d.	n.d.	11.17±0.87	0.06±0.0
WT_2	2.4±0.07	2.1±0.06	0.79±0.1	2.45±0.06	0.65±0.0	2.08±0.01	19.6±0.8	1.06±0.08	16.2±2.41	0.85±0.03
Y145A	3.0±0.08	1.45±0.08	0.79±0.04	1.61±0.02	0.94±0.03	1.56±0.08	23.4±3.66	0.63±0.07	17.27±0.15	0.57±0.01

Y145W	3.49±0.01	1.71±0.02	0.78±0.01	1.62±0.01	0.98±0.02	1.66±0.06	25.01±0.39	0.76±0.0	18.42±0.05	0.56±0.01
Q192C	3.55±0.23	1.11±0.02	0.87±0.07	1.13±0.02	1.02±0.03	1.23±0.0	24.61±0.5	0.58±0.01	16.85±0.48	0.44±0.0
Q192P	2.56±0.0	0.94±0.05	0.7±0.02	0.89±0.01	0.79±0.01	0.98±0.01	22.04±1.34	0.47±0.01	17.02±0.07	0.39±0.0
S216G	3.62±0.06	1.93±0.05	0.37±0.01	1.73±0.02	0.6±0.01	1.94±0.01	20.14±5.19	0.96±0.05	13.25±0.87	0.78±0.01
S216H	2.08±0.16	2.12±0.19	1.08±0.04	2.25±0.04	1.0±0.02	2.05±0.0	21.06±1.26	0.92±0.0	18.52±0.3	0.65±0.02
S220H	3.0±1.03	1.67±0.07	0.31±0.04	1.53±0.02	0.65±0.02	1.45±0.0	21.22±8.72	0.85±0.38	18.18±0.3	0.63±0.0
S220V	2.82±0.04	1.91±0.03	0.45±0.02	1.76±0.03	0.84±0.1	1.7±0.06	19.35±1.1	0.83±0.07	18.34±1.11	0.59±0.02
R254C	3.3±0.0	1.45±0.0	0.47±0.02	1.5±0.01	1.52±0.49	1.4±0.13	23.3±0.05	0.55±0.01	21.38±0.12	0.39±0.0
R254D	5.62±0.53	1.07±0.02	1.02±0.04	1.11±0.03	1.67±0.07	1.1±0.0	35.04±0.89	0.39±0.01	19.99±0.66	0.28±0.0
H258R	5.96±0.7	1.32±0.02	0.63±0.01	1.15±0.02	1.89±0.09	1.2±0.02	41.29±0.7	0.43±0.1	23.4±0.85	0.25±0.0
L262A	5.66±0.42	1.04±0.01	2.79±0.02	1.04±0.06	2.17±0.4	0.99±0.05	57.29±0.52	0.33±0.0	26.56±0.07	0.24±0.0
L262V	2.86±0.06	1.24±0.08	2.52±0.02	1.53±0.06	1.74±0.08	1.47±0.02	34.08±1.93	0.48±0.0	33.16±1.28	0.5±0.02
M213E S215Y	30.37±2.94	0.11±0.01	26.84±4.73	0.12±0.02	10.6±0.72	0.07±0.0	4.31±0.91	0.05±0.0	14.89±0.66	0.2±0.0
F58W S215Y	5.48±0.15	0.89±0.01	n.d.	n.d.	6.99±0.06	0.16±0.0	70.19±7.76	0.13±0.01	20.02±1.92	0.13±0.0
F58W M213E	n.d.	n.d.	n.d.	n.d.	11.81±0.27	0.14±0.0	29.92±0.63	0.13±0.0	17.36±3.88	0.08±0.0
F58W A222M	12.09±0.63	0.81±0.05	n.d.	n.d.	12.7±0.9	0.07±0.0	n.d.	n.d.	16.82±0.32	0.03±0.0
N54L H258W	23.46±3.1	0.37±0.02	0.83±0.02	0.63±0.04	1.37±0.13	0.29±0.0	56.58±7.15	0.11±0.0	24.05±1.93	0.1±0.0
T56H T93M	4.78±0.09	0.66±0.02	20.67±0.71	1.11±0.0	6.64±0.51	0.8±0.01	77.6±70.09	0.49±0.34	30.07±1.53	0.18±0.0

Supplementary Note 1. Kinetic characterization of WT-RgDAOx yeast displayed enzyme.

RgDAOx is active on a wide range of D-amino acid substrates and for each of them the enzyme exhibits a distinct set of Michaelis-Menten parameters (K_M and k_{cat}). Extending EP-Seq and tyramide assay to study the changes in RgDAOx's mutability landscape upon reaction with different substrates requires a detailed characterization of the catalytic features of the displayed enzyme. This ultimately aids selecting the optimal reaction conditions tailored to the specific substrates and ensures comparable settings among reactions. In order to investigate the properties of the displayed RgDAOx we first asked if the displayed enzyme retains the same catalytic properties of the soluble counterpart in terms of affinity and catalytic activity towards the different D-amino acids. We compared the Michaelis constant K_M of the yeast surface displayed enzyme towards different substrates to the one of its soluble counterpart expressed and purified from *Escherichia coli* BL21 cells. K_M serves as an ideal kinetic parameter for this comparison because it remains consistent regardless of the enzyme concentration tested in both systems since it is not possible to precisely quantify and therefore compare the absolute concentration of the enzyme when displayed on the yeast's surface. To this purpose, we selected nine different substrates for DAOx, including D-alanine (D-Ala), D-methionine (D-Met), D-phenylalanine (D-Phe), D-glutamine (D-Gln), D-histidine (D-His), D-threonine (D-Thr), D-asparagine (D-Asn), D-serine (D-Ser) and D-leucine (D-Leu). We assayed the activities of both yeast-displayed and soluble WT-DAOx at various substrate concentrations to determine the Michaelis-Menten K_M constant for each substrate. We detected a high degree of concordance between the K_M values calculated for the two enzymes expressed in different systems (soluble WT-DAOx vs. yeast displayed WT-DAOx, $R^2 = 0.93$) (**Supplementary Table 1**; **Supplementary Fig. 1**). This allowed us to conclude that the *Rg*DAOx enzyme displayed on the surface of the yeast strain EBY100 maintains its native state, functional properties and substrate preferences even if tethered to the cell wall through the fused Aga2 protein.

Supplementary Note 2. Selection of substrates and conditions for tyramide assay in EP-Seq.

We selected a pool of five D-amino acid substrates and experimentally determined the reaction conditions for each, ensuring the best compromise between tyramide signal and reaction incubation time at a substrate concentration equal to K_M. The five substrates, D-alanine, D-asparagine, D-methionine, D-phenylalanine, and D-glutamine exhibited high accordance in K_M values between the kinetic measurements performed with soluble and yeast-displayed forms of RgDAOx (**Supplementary Table 1**). These substrates also span a range of reaction speeds (turnover number) suitable for testing the effective performance of the tyramide assay and more importantly are characterised by diverse physical-chemical features in terms of bulkiness, polarity, and chemical composition of their side chains (**Fig. 1, Supplementary Fig. 2**). To this purpose we selected three hydrophobic substrates with distinctly different side-chain sizes and chemistries: D-alanine (D-Ala), D-phenylalanine (D-Phe), and D-methionine (D-Met). D-Ala has a small, non-polar methyl group, while D-Phe and D-Met have larger hydrophobic groups—a bulky phenyl ring in D-Phe and a thioether group with significant steric bulk in D-Met. Additionally we selected D-asparagine (D-Asn) and D-glutamine (D-Gln), two substrates with polar side chains that differ by a single CH_2 to study how polarity and size of the substrate influence activity of the RgDAOx variants. We then proceeded to carry out the tyramide assay, utilising an initial substrate concentration equivalent to K_M for each substrate, employing a mutant library of DAOx variants. This decision ensures an initial substrate concentration that prompts the reaction to operate at half of its maximum velocity, aligning with the steeper segment of the Michaelis-Menten curve. Consequently, even slight modifications to K_M or the initial reaction velocity will alter the intensity of tyramide labeling on cell surfaces, thereby enhancing the sensitivity of the assay. In contrast, the same activity assay conducted at saturating concentrations of D-alanine (V_{max}) lacks sensitivity to mutations that subtly alter K_M (but not V_{max}) towards the substrate, as they do not significantly affect the reaction velocity and the resulting tyramide signal acquired by the cells during incubation. For the tyramide assay to be conducted within the EP-Seq with the mutant library and the five substrates, we selected an incubation time of 60 minutes for hydrophobic amino acids and 120 minutes for the two polar amino acids. These incubation times, validated by using the WT-DAOx displaying cells, ensured a consistent shift towards a positive tyramide signal in all cases across the population of cells expressing the enzyme, with a median fluorescence of the fluorescent tyramide assay nearing plateau levels. Incubation times exceeding 120 minutes were avoided to prevent cell precipitation and nonspecific tyramide signaling in the negative population (**Supplementary Fig. 2**).